Wave-vector- and frequency-dependent dielectric matrix for aluminum: Energy-loss spectra*

S. P. Singhal
Department of Physics and Astronomy, Louisiana State University, Baton Rouge, Louisiana 70803
(Received 29 March 1976)

A previous calculation of the dielectric matrix in aluminum in the static limit is extended to include the frequency dependence. Exchange and correlation corrections to the random-phase results are studied according to three different approximations. The values of $\mathrm{Im}[\epsilon^{-1}(k,\omega)]_{11}$, responsible for the electron-energy-loss cross sections, are computed and compared with the experimental results of Petri and Otto. The results do not depend significantly on the form of exchange-correlation corrections employed.

I. INTRODUCTION

In a recent paper,[1] we studied the dielectric matrix for aluminum in the static limit ($\omega = 0$). However, important information is contained in the ω-dependent quantity, e.g., the electron-energy-loss cross section depends on the imaginary part of the dielectric response function

$$R = [\,\hat{p}\cdot\vec{\epsilon}\,(\vec{p},\omega)\cdot\hat{p}\,]^{-1}, \tag{1}$$

where $\vec{\epsilon}(\vec{p},\omega)$ is the dielectric matrix for fields of wave vector $\vec{p}$ and frequency ω.

The equations derived in I for the static dielectric matrix are extended to include ω in the random-phase approximation (RPA). As before, the Bloch states are expanded in terms of a set of Gaussian functions, and numerical results are obtained for the wave-vector and frequency-dependent dielectric matrix.

Three forms of exchange-correlation correction to the RPA results are studied. The first is determined from a self-consistent treatment of the dielectric matrix using the local exchange ($X\alpha$) Hamiltonian.[2] The second is that given by Toigo and Woodruff,[3] (TW) and the third, that of Vashishta and Singwi.[4]

Section II gives the basic equations for the p,ω-dependent dielectric matrix along with the proper corrections to the RPA result. The numerical results are presented in Sec. III, and compared with the experimental data of Petri and Otto,[5] and show very good agreement. It is also seen that the band structure plays a major role in the peak positions of the cross section versus energy curves.

II. FORMALISM

The dielectric response was described in I for zero frequency by the equation (in the RPA)

$$\epsilon_{ts}(\vec{p}) = \epsilon(\vec{p}+\vec{K}_t, \vec{p}+\vec{K}_s) = \delta_{st} - v_c(\vec{p}+\vec{K}_t)\chi_{ts}(\vec{p}), \tag{2}$$

where $\vec{K}_s, \vec{K}_t$ are reciprocal-lattice vectors, and $v_C(\vec{p}+\vec{K}_t)$ is the Fourier transform of the Coulomb potential, given by

$$v_C(\vec{p}+\vec{K}_t) = 4\pi e^2/(\vec{p}+\vec{K}_t)^2. \tag{3}$$

The irreducible polarization part of the density response matrix χ_{ts} is given by

$$\chi_{ts}(\vec{p}) = \frac{2}{N\Omega}\sum_{n\vec{k},l\vec{q}} \frac{N_n(\vec{k}) - N_l(\vec{q})}{E_n(\vec{k}) - E_l(\vec{q})} \times\langle l\vec{q}|\, e^{i(\vec{p}+\vec{K}_s)\cdot\vec{r}}\,|n\vec{k}\rangle \times\langle n\vec{k}|\, e^{-i(\vec{p}+\vec{K}_t)\cdot\vec{r}}\,|l\vec{q}\rangle, \tag{4}$$

where $E_n(\vec{k})$ and $N_n(\vec{k})$ are the energy and the occupation number, respectively, of an electron of momentum $\vec{k}$ and band n; $|n\vec{k}\rangle$ is the Bloch state for such an electron; and N is the number of unit cells of volume Ω each. We have explicitly included a factor of 2 in Eq. (4) to account for both spins. The quantity χ_{ts} defined in (4) is $2/\Omega$ times Q_{ts} used in I.

The expression for $\chi_{ts}(\vec{p})$ was given in terms of a surface integral

$$\chi_{ts}(\vec{p}) = \frac{2}{(2\pi)^3}\sum_{nl}\sum_{\alpha}\int\frac{dE}{E}\int ds\,\frac{N_n(\vec{q}-\alpha^{-1}\vec{p}) - N_l(\vec{q})}{|\,\mathrm{grad}\Delta_{nl}(\vec{q},\alpha^{-1}\vec{p})|}\sum_{\gamma} m_{ln}(\alpha^{-1}\gamma^{-1}\vec{p}_s,\vec{q})\,m^*_{ln}(\alpha^{-1}\gamma^{-1}\vec{p}_t,\vec{q}), \tag{5}$$

where

$$\Delta_{nl}(\vec{q},\alpha^{-1}\vec{p}) = E_n(\vec{q}-\alpha^{-1}\vec{p}) - E_l(\vec{q}), \tag{6}$$

and the surface integral is over all $\vec{q}$ within the irreducible subzone satisfying the condition $\Delta_{nl} = E$.

The matrix elements m_{ln} are defined by

$$\langle l\vec{q}|\, e^{i\vec{p}_s\cdot\vec{r}}\,|n\vec{k}\rangle = m_{ln}(\vec{p}_s,\vec{q})\delta_{\vec{k},(\vec{q}-\vec{p})}, \tag{7}$$

where $\vec{p}_s$ is the shorthand notation for $\vec{p}+\vec{K}_s$. It is understood in Eqs. (5)–(7) that if $\vec{q}-\vec{p}$ lies out-

side the Brillouin zone, it is to be brought back into it by the subtraction of a reciprocal-lattice vector. The operators γ and α belong to the cubic group such that

$$\gamma\vec{p}=\vec{p}, \quad \alpha\vec{p}=\vec{p}', \tag{8}$$

where $\vec{p}'$ is a member of the star of $\vec{p}$. The evaluation of a vast number of the matrix elements m_{ln} is reduced by the use of the transformation relations

$$m_{ln}(\vec{p}_s, \beta\vec{q}) = (x)\, m_{ln}(\beta^{-1}\vec{p}_s, \vec{q}), \tag{9a}$$

where x represents a phase factor. As shown in I, these phase factors cancel out in the expression for $\chi_{ts}(\vec{p})$ if the matrix elements are calculated by a special prescription using the m'_{ln} matrix defined by (A12) of I.

The number of independent matrix elements is further reduced by the relation (not used in I)

$$m_{ln}(\vec{p}_s, \vec{q}) = (x)\, m_{nl}(\vec{p}_s, \vec{p}_s - \vec{q}), \tag{9b}$$

where x is again a phase factor and $\vec{p}_s - \vec{q}$ is to be brought back to the Brillouin zone, if needed.

The dielectric response to an applied field of momentum $\vec{p}$ and frequency ω is the extension of (2) in the form

$$\epsilon_{ts}(\vec{p}, \omega) = \delta_{st} - v_C(\vec{p}+\vec{K}_t)\chi_{ts}(\vec{p}, \omega), \tag{10}$$

where

$$\chi_{ts}(\vec{p}, \omega) = \frac{2}{N\Omega} \sum_{\substack{n\vec{k} \\ l\vec{q}}} \frac{N_n(\vec{k}) - N_l(\vec{q})}{E_n(\vec{k}) - E_l(\vec{q}) - \hbar\omega^+} \times \langle l\vec{q}|\, e^{i\vec{p}_s\cdot\vec{r}}\,|n\vec{k}\rangle \times \langle n\vec{k}|\, e^{-i\vec{p}_t\cdot\vec{r}}\,|l\vec{q}\rangle \tag{11}$$

and

$$\omega^+ = \lim_{\eta\to 0}(\omega + i\eta), \tag{12}$$

to satisfy the proper causality relations (this leads to $\chi_{ts}(\vec{p}, \omega)$ being analytic in the upper half-plane). The imaginary part of χ_{ts} has the energy δ function leading to an expression quite similar to Eq. (5), but without the energy integral

$$\mathrm{Im}\chi_{ts}(\vec{p}, \omega) = (\pi)\frac{2}{(2\pi)^3} \sum_{nl} \sum_{\alpha} \int ds \frac{N_n(\vec{q} - \alpha^{-1}\vec{p}) - N_l(\vec{q})}{|\,\mathrm{grad}\Delta_{nl}(\vec{q}, \alpha^{-1}\vec{p})|} \sum_{\gamma} m_{ln}(\alpha^{-1}\gamma^{-1}\vec{p}_s, \vec{q})\, m^*_{tn}(\alpha^{-1}\gamma^{-1}\vec{p}_t, \vec{q}), \tag{13}$$

and the surface integral is over all $\vec{q}$ within the subzone satisfying the condition $\Delta_{nl} = \hbar\omega$. The real part of χ_{ts} is the Hilbert transform, given by the principal-value integral

$$\mathrm{Re}\chi_{ts}(\vec{p}, \omega) = \left(\frac{1}{\pi}\right) \mathrm{P} \int \frac{\mathrm{Im}\chi_{ts}(\vec{p}, \omega')}{\omega' - \omega}\, d\omega'. \tag{14}$$

The polarization $\chi_{ts}(\vec{p}, \omega)$ possesses certain symmetry properties given by

$$\chi_{ts}(\vec{p}, \omega) = \chi_{st}(\vec{p}, \omega), \tag{15}$$

$$\chi_{t's'}(\vec{p}, \omega) = \chi_{ts}(\vec{p}, \omega), \tag{16}$$

where $\vec{p}+\vec{K}_{t'}$ and $\vec{p}+\vec{K}_{s'}$ are connected to $\vec{p}+\vec{K}_t$ and $\vec{p}+\vec{K}_s$, respectively, by the same operator γ, and

$$\chi_{ts}(\vec{p}, -\omega) = \chi^*_{s''t''}(-\vec{p}, \omega), \tag{17}$$

where

$$\vec{K}_{s''} = -\vec{K}_s, \quad \vec{K}_{t''} = -\vec{K}_t,$$

and finally,

$$\chi_{ts}(\vec{p}, -\omega) = \chi^*_{st}(\vec{p}, \omega). \tag{18}$$

The dielectric matrix in the RPA is thus given by

$$\epsilon(\vec{p}, \omega) = \vec{I} + Q^{(0)}(\vec{p}, \omega), \tag{19}$$

where

$$Q^{(0)}(\vec{p}, \omega) = -v_C(\vec{p})\chi(\vec{p}, \omega). \tag{20a}$$

$\chi(\vec{p}, \omega)$ is the matrix given by Eq. (11) and $v_C(\vec{p})$ is the diagonal matrix

$$[v_C(\vec{p})]_{st} = v_C(\vec{p}+\vec{K}_s)\delta_{st}. \tag{20b}$$

Equation (19) must be corrected for exchange and correlation effects. One such correction involves the self-consistent treatment of the dielectric matrix using the local exchange Hamiltonian,[2] and yields the result

$$\epsilon(\vec{p}, \omega) = \vec{I} + Q^{(0)}(\vec{p}, \omega)[\vec{I} - v_x\chi(\vec{p}, \omega)]^{-1}, \tag{21}$$

where

$$(v_x)_{st} = v_x(\vec{K}_s - \vec{K}_t) = \left(\frac{c}{3}\right)\frac{1}{\Omega}\int \rho_0^{-2/3}(\vec{r})e^{i(\vec{K}_s - \vec{K}_t)\cdot\vec{r}}\, d^3r, \tag{22a}$$

$$C = (-6\alpha)\left(\frac{3}{8\pi}\right)^{1/3}, \tag{22b}$$

and α is the exchange parameter (value $\frac{2}{3}$ as used in the band-structure calculation for aluminum), and $\rho_0(\vec{r})$ is the charge density available from the self-consistent band-structure calculation.

The correction described above includes the exchange effects self consistently. However, the correlation effects are included only to the extent of cancelling the divergent terms of the pure exchange.[6] Many authors have included both the exchange and correlation effects in the form of a function $G(\vec{p})$[7] which modifies the RPA dielectric

matrix in a manner similar to Eq. (21), e.g.,

$$\epsilon(\vec{p},\omega)=\vec{I}+Q^{(0)}(\vec{p},\omega)[\vec{I}-\mathcal{G}(\vec{p})Q^{(0)}(\vec{p},\omega)]^{-1}, \tag{23}$$

where $\mathcal{G}(\vec{p})$ is the diagonal matrix

$$[\mathcal{G}(\vec{p})]_{st}=G(\vec{p}+\vec{K}_s)\delta_{st}. \tag{24}$$

The results presented in I [Eqs. (36a) and (36b) of I] are the approximate forms of Eq. (23), where the correction factor $(1-\mathcal{G}Q^{(0)})^{-1}$ is assumed to be diagonal. This approximation bears out quite well, at least in the present case, where $[\epsilon^{-1}(\vec{p},\omega)]_{11}$ [matrix element for $\vec{K}_s=\vec{K}_t=(0,0,0)$] was computed using both Eq. (23) and the approximate form used in I.

III. RESULTS

In I, we reported the results for $\chi_{ts}(\vec{p})$ for three principal directions, Δ, Σ, and Λ, for a total of nine values of $\vec{p}$. The numerical integrations were performed by using four-point division along the Δ line (i.e., dividing the Brillouin zone into a cubic mesh with four divisions along the $\Gamma-X$ line. This gives 20 points in the irreducible part of the Brillouin zone). Prompted by the concern expressed by Harmon[8] as to the accuracy of this integration, we performed some checks of the symmetry relation (18) for a few values of ω, both with and without the use of matrix elements m_{in} in Eq. (13). It turns out that in the four-division case, the relation (18) is not properly satisfied [errors of (10–20)% were quite common], indicating that the band-structure effects must be

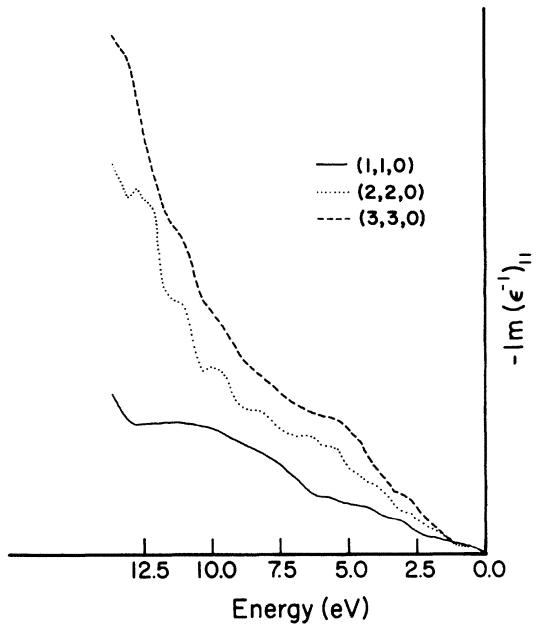

FIG. 2. Energy-loss cross sections for $\vec{p}$ along Σ direction.

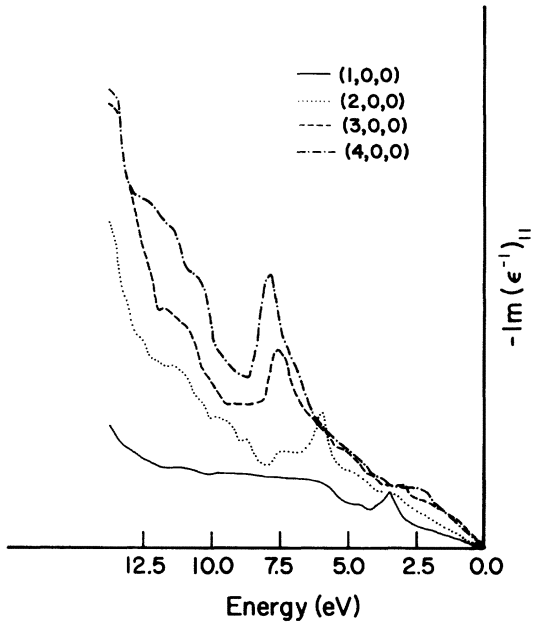

FIG. 1. Energy-loss cross sections: plot of $-\mathrm{Im}[\epsilon^{-1}(\vec{p},\omega)]_{11}$ (arbitrary scale) vs energy loss (ω) in eV for $\vec{p}$ along the Δ direction. Curves are drawn for different values of $\vec{p}$ shown in units of $\pi/2a$. The symbolism is shown.

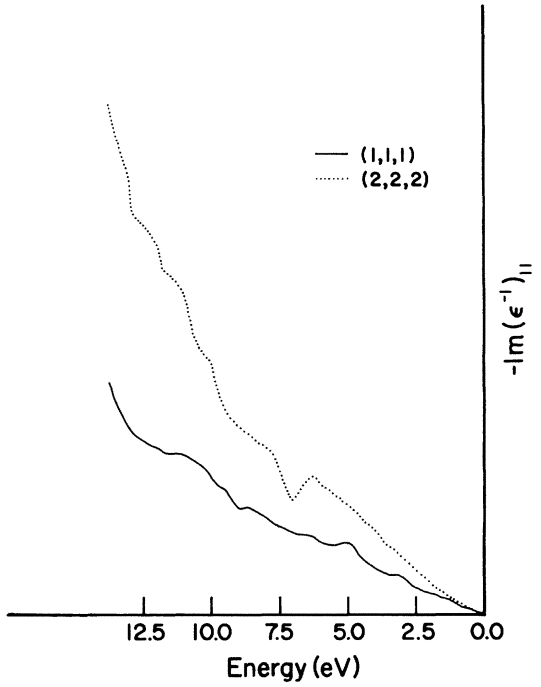

FIG. 3. Energy-loss cross sections for $\vec{p}$ along Λ direction.

included for a finer mesh. The eight-division case (leading to 89 points in the irreducible zone) satisfied relation (18) to within 5% or less for most points checked. Since the matrix elements m_{ln} are fairly smoothly varying compared to the band structure, and take extremely long to compute, the calculations were performed by using eight-division bands, but the m_{ln}'s interpolated from the four-division results [to avoid the problem with the phase factors, it was really the expression $\sum_\gamma m_{ln}(\vec{p}_s) m^*_{ln}(\vec{p}_t)$, that was interpolated].

We used 15 values for the reciprocal-lattice vectors $\vec{K}_s$ and $\vec{K}_t$ [all members of the stars of (0, 0, 0), (1, 1, 1) and (2, 0, 0)], and evaluated the 15×15 matrix $\chi(\vec{p}, \omega)$, and finally the matrices $\epsilon(\vec{p}, \omega)$ and $\epsilon^{-1}(\vec{p}, \omega)$. The values of $\mathrm{Im}[\epsilon^{-1}(\vec{p}, \omega)]_{11}$, the matrix element for $K_s = K_t = (0, 0, 0)$, are plotted against the energy $\hbar\omega$ (in eV) in Figs. 1–3 for p along Δ, Σ, and Λ, directions, respectively. Values of $G(\vec{p})$ for exchange and correlation corrections were obtained from TW.[3] Calculations were repeated for $G(\vec{p})$ given by Vashishta and Singwi[4] ($r_s = 2$ values, applicable to aluminum), and the two sets of results were found to agree remarkably well.

Figure 4 shows the comparison of four-division and eight-division results for the four values of $\vec{p}$ along the Δ direction, which clearly shows the inadequacy of the four-division results if the energy dependence of the response matrix is desired. However, the values of $\chi_{ts}(\vec{p}, \omega = 0)$ seem to agree fairly well in the two cases [within (5–10)%], as reported in I.

Figure 5 shows the energy-loss cross sections in RPA [no correction to Eq. (19)] for three points

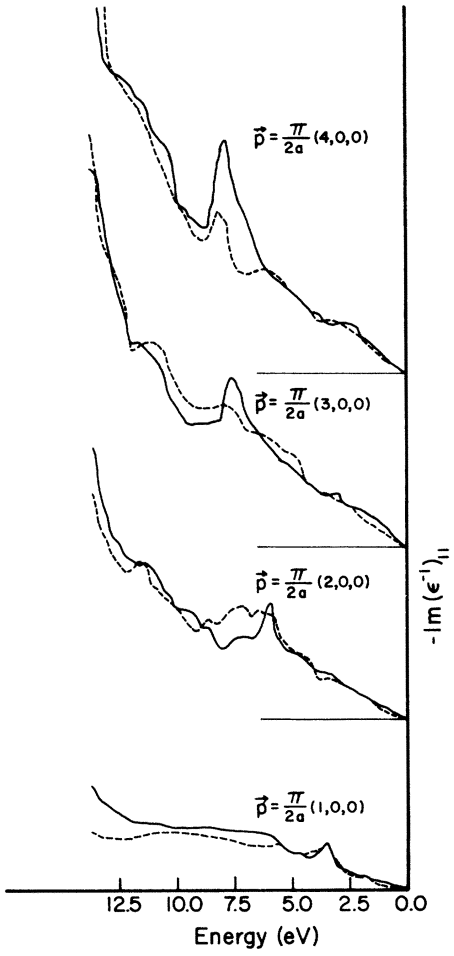

FIG. 4. Energy-loss curves for $\vec{p}$ along the Δ direction; effect of using the band structure for a finer mesh of points in the k-space integral. The mesh size used to compute the solid curves was half the mesh size used for the dashed curves.

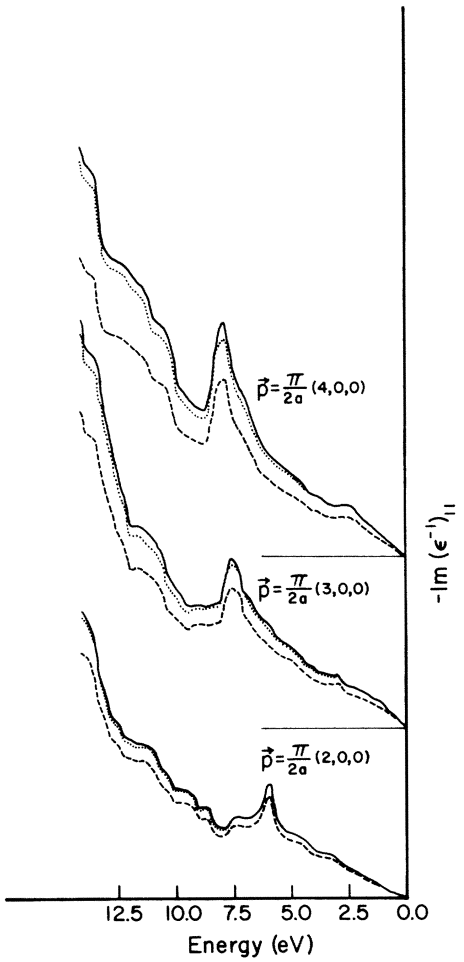

FIG. 5. Energy-loss curves for $\vec{p}$ along the Δ direction. RPA results (dashed curves) compared with those corrected by $X\alpha$ exchange (dotted curves), and by the Toigo and Woodruff correction factor (solid curves).

TABLE I. Peak positions in the energy-loss curves for $\vec{k}$ in the three principal directions Δ, Σ, and Λ.

	Present work		Expt. Ref. 5		
$\hat{k}$	k (Å^{-1})	E(eV)	k (Å^{-1})	E(eV) (700-Å film)	E(eV) (1000-Å film)
[100]	0.39	3.6	0.44	8.9	3.8
	0.78	6.0,7.4,8.6,11.2	0.74		5.7,7.9
			0.80	6.1,8.7	
	1.17	7.5,11.6	0.87	6.5,10.0	
			0.99		7.3,11.6
	1.56	7.8			
[110]	0.55	3.0–5.8	0.55		3.4–6.6
			0.58	3.5–6.8	
	1.10	5.3–6.4,8.4,10.0	0.81		6.5–8.5
			0.87	6.7–8.7	
	1.65	5.5			
[111]	0.67	5.2,8.6	0.65	5.8	
			0.66		6.1
	1.35	6.2			

in the Δ direction. The exchange correction, consistent with the $X\alpha$ approximation, was applied according to Eq. (21). The correction matrix v_x was evaluated using the charge density of a lattice of neutral aluminum atoms in the $1s^2 2s^2 2p^6 3s^2 3p^1$ configuration.[9] This is the charge density that was used as an input to the self-consistent band calculation,[10] and not the self-consistent charge density resulting from the band calculation. However, since the exchange correction to the dielectric matrix is small, this difference in the charge density can be easily ignored. The results of the $X\alpha$ correction are compared in Fig. 5 with the RPA results, and those corrected by the TW values of $G(p)$ including exchange and correlation. It is observed that all three cases give the same peak positions in the energy-loss spectra, indicating that the major structure is that due to the band structure, and not a manifestation of the different exchange-correlation corrections to the RPA result. Furthermore, the $X\alpha$ curves fall between the RPA and TW corrected results, as expected due to the fact that it includes only the exchange part of the correction. For other values of $\vec{p}$ (not shown in Fig. 5), the results are quite similar in nature.

Petri and Otto[5] have reported experimental measurements of the energy-loss spectra in aluminum films of thicknesses 700 and 1000 Å. Their published results are reported in graphical form. We cannot compare our results directly with theirs because we can make calculations for $\vec{p}$ of the type $(\pi/2a)(n_1, n_2, n_3)$, only. The energy resolution of their experiments is 0.7 eV, which is approximately double the energy separation (0.02 Ry) used in the calculations. The comparison for the peak positions for approximately comparable values of $\vec{p}$ is shown in Table I, which shows excellent agreement for Δ direction, where the peaks are much more pronounced than in the other two directions.

In conclusion, we observe that a detailed calculation of the dielectric matrix with the self-consistent bands and wave functions provides a good explanation of the electron-energy-loss results. Most of the structure comes from the band effects, indicating the need for accurate band-structure calculations in computing energy-loss spectra. Since the three forms of exchange-correlation corrections do not differ very much, more precise experimental data will be required to distinguish between different theoretical approximations.

ACKNOWLEDGMENTS

The author wishes to thank Professor J. Callaway for many helpful discussions. Thanks are also due to Dr. E. Petri for providing some of the detailed results of the experiment (Ref. 5).

*Work supported by the U. S. Army Research Office, Research Triangle Park, N. C.

[1]S. P. Singhal, Phys. Rev. B 12, 564 (1975); 12, 6007(E) (1975); referred to as I.

[2]S. P. Singhal and J. Callaway, preceding paper, Phys. Rev. B 14, 2347 (1976).

[3]F. Toigo and T. O. Woodruff, Phys. Rev. B 2, 3958 (1970); 4, 371 (1971).

[4]P. Vashishta and K. S. Singwi, Phys. Rev. B 6, 875 (1972).

[5]E. Petri and A. Otto, Phys. Rev. Lett. 34, 1283 (1975); and private communication.

[6]K. J. Duff and A. W. Overhauser, Phys. Rev. B 5, 2799 (1972).

[7]For a recent review of methods used the $G(p)$ type correction, see A. A. Kugler, J. Stat. Phys. 12, 35 (1975).

[8]B. Harmon (private communication).

[9]E. Clementi and C. Roetti, At. Data Nucl. Data Tables, 14, 177 (1974).

[10]R. A. Tawil and S. P. Singhal, Phys. Rev. B 11, 699 (1975).